bioRxiv preprint doi: https://doi.org/10.1101/319228; this version posted May 14, 2018. The copyright holder for this preprint (which was not certified by peer review) is the author/funder. All rights reserved. No reuse allowed without permission.

1 # *Escherichia coli* ZipA organizes FtsZ polymers into dynamic ring-like
2 protofilament structures
3
4 Marcin Krupka[1]*, Marta Sobrinos-Sanguino[2*], Mercedes Jiménez[2], Germán Rivas[2], and
5 William Margolin[1]
6
7 [1]Department of Microbiology and Molecular Genetics, McGovern Medical School, 6431
8 Fannin St., Houston TX, 77030, USA.
9
10 [2]Centro de Investigaciones Biológicas, Consejo Superior de Investigaciones Científicas
11 (CSIC), C/ Ramiro de Maetzu 9, 28040, Madrid, Spain.
12
13
14 (*) These authors contributed equally
15
16 Corresponding Authors:
17 William Margolin
18 Mercedes Jiménez
19 Germán Rivas
20
21
22
23
24

bioRxiv preprint doi: https://doi.org/10.1101/319228; this version posted May 14, 2018. The copyright holder for this preprint (which was not certified by peer review) is the author/funder. All rights reserved. No reuse allowed without permission.

1 **ABSTRACT**

2 ZipA is an essential cell division protein in *Escherichia coli*. Together with FtsA, ZipA
3 tethers dynamic polymers of FtsZ to the cytoplasmic membrane, and these polymers are
4 required to guide synthesis of the cell division septum. This dynamic behavior of FtsZ has
5 been reconstituted on planar lipid surfaces *in vitro*, visible as GTP-dependent chiral vortices
6 several hundred nm in diameter, when anchored by FtsA or when fused to an artificial
7 membrane binding domain. However, these dynamics largely vanish when ZipA is used to
8 tether FtsZ polymers to lipids at high surface densities. This, along with some *in vitro* studies
9 in solution, has led to the prevailing notion that ZipA reduces FtsZ dynamics by enhancing
10 bundling of FtsZ filaments. Here, we show that this is not the case. When lower, more
11 physiological levels of the soluble, cytoplasmic domain of ZipA (sZipA) were attached to
12 lipids, FtsZ assembled into highly dynamic vortices similar to those assembled with FtsA or
13 other membrane anchors. Notably, at either high or low surface densities, ZipA did not
14 stimulate lateral interactions between FtsZ protofilaments. We also used *E. coli* mutants that
15 are either deficient or proficient in FtsZ bundling to provide evidence that ZipA does not
16 directly promote bundling of FtsZ filaments *in vivo*. Together, our results suggest that ZipA
17 does not dampen FtsZ dynamics as previously thought, and instead may act as a passive
18 membrane attachment for FtsZ filaments as they treadmill.

19

20

bioRxiv preprint doi: https://doi.org/10.1101/319228; this version posted May 14, 2018. The copyright holder for this preprint (which was not certified by peer review) is the author/funder. All rights reserved. No reuse allowed without permission.

1 **IMPORTANCE**

2 Bacterial cells use a membrane-attached ring of proteins to mark and guide formation of a
3 division septum at mid-cell that forms a wall separating the two daughter cells and allows
4 cells to divide. The key protein in this ring is FtsZ, a homolog of tubulin that forms dynamic
5 polymers. Here, we use electron microscopy and confocal fluorescence imaging to show that
6 one of the proteins required to attach FtsZ polymers to the membrane during *E. coli* cell
7 division, ZipA, can promote dynamic swirls of FtsZ on a lipid surface *in vitro*. Importantly,
8 these swirls are only observed when ZipA is present at low, physiologically relevant surface
9 densities. Although ZipA has been thought to enhance bundling of FtsZ polymers, we find
10 little evidence for bundling *in vitro*. In addition, we present several lines of *in vivo* evidence
11 indicating that ZipA does not act to directly bundle FtsZ polymers.

12

13

bioRxiv preprint doi: https://doi.org/10.1101/319228; this version posted May 14, 2018. The copyright holder for this preprint (which was not certified by peer review) is the author/funder. All rights reserved. No reuse allowed without permission.

1 **INTRODUCTION**

2 Bacterial septation is a complex process and dozens of essential and accessory
3 proteins participate to assemble the cell division machinery, the divisome. In *Escherichia coli*
4 the earliest event in the septum formation is the assembly of FtsZ, FtsA and ZipA into the
5 proto-ring, a discontinuous structure at mid-cell that serves as a scaffold for the rest of the
6 divisome components (1, 2).

7 FtsZ, a prokaryotic tubulin homologue, assembles into GTP-dependent protofilaments
8 required for divisome activity (3–7). These FtsZ filaments are anchored to the inner surface
9 of the cytoplasmic membrane by both FtsA and ZipA, and migrate in patches around the cell
10 circumference by treadmilling. Through connections involving other divisome proteins that
11 cross the cytoplasmic membrane, these treadmilling FtsZ protofilaments help to guide the
12 septum synthesis machinery in concentric circles, resulting in inward growth of the septal
13 wall until it closes and the daughter cells are separated (8, 9).

14 Although FtsA is conserved throughout diverse bacterial species, ZipA is limited to
15 gamma-proteobacteria, including *E. coli* (10). In the absence of both FtsA and ZipA, FtsZ
16 fails to attach to the membrane or form the proto-ring, demonstrating the requirement for a
17 membrane tether (11). In the presence of only FtsA or ZipA, FtsZ filaments form a
18 membrane-anchored ring, but septation fails to proceed (12), suggesting that the divisome is
19 in a locked state. One major unanswered question in the field is why *E. coli* requires dual
20 FtsZ membrane anchors to assemble a divisome that completes septation. Our recent study
21 provides a potential answer by showing that FtsA exerts a specific structural and functional
22 constraint on FtsZ protofilaments: when attached to lipid monolayers, FtsA assembles into
23 clusters of polymeric minirings that align FtsZ polymers and inhibit their bundling (13).

24 In this report we use the term "bundling" in reference to increased lateral interactions
25 between adjacent FtsZ protofilaments, resulting in two or more polymers closely associated

bioRxiv preprint doi: https://doi.org/10.1101/319228; this version posted May 14, 2018. The copyright holder for this preprint (which was not certified by peer review) is the author/funder. All rights reserved. No reuse allowed without permission.

1 in parallel. The physiological role of these lateral interactions is not firmly established, but
2 several FtsZ mutants that are defective in protofilament bundling *in vitro* are also defective in
3 cell division (14–16). In addition to the intrinsic ability of FtsZ polymers to interact laterally,
4 proteins called Zaps (ZapA, C, D; FtsZ-associated proteins) help to bundle or crosslink FtsZ
5 polymers *in vitro* (17, 18). Inactivation of single Zap proteins is not lethal, but mutant cells
6 lacking multiple Zap proteins have significant division defects (19–23). Hyper-bundled
7 mutants of FtsZ have also been isolated, and cells expressing these alleles also divide
8 abnormally (24–26). However, one hyper-bundling mutant, called FtsZ*, has gain-of-
9 function properties (27). FtsZ*, which forms mostly double stranded filaments *in vitro*,
10 allows division of cells lacking ZipA and can resist the effects of other FtsZ inhibitors.
11 Together, these findings suggest that lateral interactions are important for FtsZ function, but
12 these interactions need to be balanced.

13 The aforementioned study (13) proposed a model in which FtsA minirings antagonize
14 FtsZ protofilament bundling, keeping the divisome in a locked state. In this model, once the
15 cell is ready to divide, these minirings are disrupted and are no longer a constraint for FtsZ
16 polymer bundling. This is consistent with another model in which broken FtsA polymers start
17 to recruit later divisome components, while FtsZ polymers become anchored to cell
18 membrane by ZipA (2, 28). ZipA has been shown to stabilize the proto-ring, not only by
19 anchoring FtsZ to the membrane, but also by protecting it from degradation by ClpXP
20 protease (29–31). Whereas FtsA inhibits FtsZ polymer bundling (13), ZipA is considered an
21 FtsA competitor for FtsZ polymers because of their common binding site at the FtsZ C
22 terminus (32–35). Thus, it is not surprising that ZipA has been suggested as a bundler of
23 FtsZ. However, the reports on its effect on FtsZ protofilament bundling in solution are not
24 consistent (27, 36–40).

bioRxiv preprint doi: https://doi.org/10.1101/319228; this version posted May 14, 2018. The copyright holder for this preprint (which was not certified by peer review) is the author/funder. All rights reserved. No reuse allowed without permission.

1 Recently it has become clear that the functionalities of the proto-ring proteins need to
2 be tested in a more physiological context by attaching them to a lipid surface (13, 41–47).
3 For example, Mateos-Gil et al. (39) used atomic force microscopy to visualize FtsZ polymers
4 bound to *E. coli* lipid bilayers through ZipA. These ZipA-tethered FtsZ molecules formed a
5 dynamic two-dimensional network of curved, interconnected protofilaments that seemed to
6 be bundled. On the contrary, ZipA incorporated into phospholipid bilayer nanodiscs did not
7 trigger significant FtsZ polymer bundling (29). Finally, Loose and Mitchison (44)
8 reconstituted the *E. coli* proto-ring components on supported lipid bilayers and showed that
9 FtsA organized FtsZ polymers into dynamic patterns of coordinated streams and swirling
10 rings with preferential directions, which suggested treadmilling. Importantly, these dynamics
11 were sharply reduced when FtsZ protofilaments were attached to the membrane by ZipA or
12 when using artificially membrane-targeted FtsZ. Although the resulting FtsZ polymers were
13 described as bundled, the resolution obtained by TIRFM probably could not distinguish
14 between single and bundled FtsZ protofilaments. More recently, it was found that artificially
15 membrane-bound FtsZ self-organizes into similar vortices, even in the absence of FtsA (45).
16 This effect casts doubt on the dampening effects of ZipA on FtsZ dynamics observed
17 previously.
18 In this study, we revisit the effect of ZipA on FtsZ protofilaments, including its role in
19 polymer bundling. In contrast to the prevailing model, our *in vivo* results show that unlike
20 Zaps, FtsZ* or the FtsA* gain of function mutant (48), ZipA does not play a significant role
21 in FtsZ protofilament bundling. We further show that as previously reported (46, 49)
22 (Sobrinos-Sanguino et al., in preparation), the surface concentration of ZipA is critical in
23 controlling the activities and interactions with FtsZ *in vitro*. Using a His_6-tagged soluble
24 variant of ZipA (sZipA) immobilized on lipids, we demonstrate that this protein organizes
25 FtsZ into similar swirling vortices of mostly single protofilaments, a role that was previously

bioRxiv preprint doi: https://doi.org/10.1101/319228; this version posted May 14, 2018. The copyright holder for this preprint (which was not certified by peer review) is the author/funder. All rights reserved. No reuse allowed without permission.

attributed exclusively to FtsA (44). These results provide further evidence that ZipA does not inhibit FtsZ polymer dynamics at the membrane.

RESULTS

FtsA* or excess FtsZ rescue the FtsZ bundling deficient Δ*zapA*Δ*zapC* mutant

Recently we reported that FtsZ protofilament bundling is antagonized by FtsA, both *in vivo* and *in vitro* (13). For example, FtsA overproduction reverses the toxic effects of FtsZ over-bundling triggered by excess ZapA. Conversely, even a slight excess of FtsA exacerbates the already moderately filamentous cell phenotype of Δ*zapA* or the more severe filamentous phenotype of Δ*zapA*Δ*zapC* double mutants (13), which lack one or two FtsZ bundling proteins, respectively (18). We also previously reported that the self-bundling mutant *ftsZ** (encoding (FtsZ$_{L169R}$) could completely suppress the cell division deficiency of the Δ*zapA*Δ*zapC* double mutant (27). This suggested that if FtsZ protofilaments are bundled by factors independent of ZapA and ZapC, then the requirement for the latter proteins in normal cell division could be bypassed.

We first surmised that a moderate increase in intracellular FtsZ concentration could promote polymer bunding simply by molecular crowding, and this could bypass the need for ZapA and ZapC and consequently suppress the filamentation of many Δ*zapA*Δ*zapC* cells (Fig. 1A-B). To produce extra FtsZ, we used the pJF119HE-FtsZ plasmid (26). As expected, FtsZ overproduction suppressed Δ*zapA*Δ*zapC* cell filamentation (Fig. 1C), supporting the idea that higher FtsZ protein concentration favors increased lateral interactions between protofilaments.

We then asked whether FtsA*, a potent gain-of-function mutant that repairs multiple cell division defects (48, 50–53), could bypass the need for ZapA and ZapC. Unlike wild-

bioRxiv preprint doi: https://doi.org/10.1101/319228; this version posted May 14, 2018. The copyright holder for this preprint (which was not certified by peer review) is the author/funder. All rights reserved. No reuse allowed without permission.

1 type FtsA, FtsA* promotes FtsZ polymer bundling on lipid monolayers (13). We found that
2 even uninduced levels of FtsA* from pDSW210F-FtsA* were sufficient to completely rescue
3 the division defects of Δ*zapA*Δ*zapC* cells (Fig. 1D). Therefore, FtsA* has the same rescuing
4 effect as FtsZ* in the absence of ZapA and ZapC, supporting the idea that FtsA*, ZapA and
5 ZapC all promote FtsZ protofilament bundling like FtsZ*.
6
7 **Excess ZipA cannot counteract cell division defects caused by deficient FtsZ bundling**
8 As already mentioned, *E. coli* FtsA inhibits FtsZ polymer bundling. Our *in vitro*
9 results indicate that this occurs due to the unusual mini-ring polymers that purified FtsA
10 forms on lipid monolayers. In contrast, purified FtsA* forms shorter curved oligomers under
11 similar conditions. Although the mechanism is not yet known, these FtsA* arcs no longer
12 inhibit FtsZ polymer bundling and instead permit or promote it, consistent with our *in vivo*
13 results (Fig. 1D). This was most apparent when FtsA* was combined with FtsZ* on lipid
14 monolayers: in a striking additive effect, large sheets were formed consisting of many
15 laterally associated protofilaments (13). Interestingly, both gain of function mutants that
16 promote FtsZ bundling, FtsA* and FtsZ*, bypass the need of the third proto-ring component,
17 ZipA (27, 48). This, along with evidence that purified ZipA can bundle FtsZ under certain
18 conditions, led to the hypothesis that ZipA might also trigger FtsZ bundling (54).
19 In this scenario, excess ZipA should be able to rescue the Δ*zapA*Δ*zapC* cell filamentation
20 phenotype, similarly to excess FtsZ, FtsA* or FtsZ* (27) (Fig. 1). To test this, we first
21 transformed the Δ*zapA*Δ*zapC* double deletion and its TB28 wild-type parental strain (55)
22 with pKG110-ZipA, a plasmid that expresses *zipA* from a salicylate-inducible *nahG* promoter
23 and a weak ribosome binding site that keeps expression low. Notably, uninduced levels of
24 ZipA from pKG110-ZipA did not suppress the Δ*zapA*Δ*zapC* filamentous phenotype (Fig.
25 2B). Instead, the induction of *zipA* expression was consistently more toxic not only for

bioRxiv preprint doi: https://doi.org/10.1101/319228; this version posted May 14, 2018. The copyright holder for this preprint (which was not certified by peer review) is the author/funder. All rights reserved. No reuse allowed without permission.

1 Δ*zapAzapC,* but also for the Δ*zapA* single deletion strain when compared with the wild-type
2 parent TB28 (Fig. 2A). Endogenous FtsZ was produced at similar levels in both ZipA-
3 uninduced and induced cells, ruling out the possibility that excess ZipA could affect viability
4 through changes in FtsZ intracellular levels (Fig. S1A).

5 Further growth until late exponential phase exacerbated the already elongated cell
6 phenotype of the Δ*zapA*Δ*zapC* strain both in the absence (Fig. 2C) and presence of inducer
7 (Fig. 2D); cells of the Δ*zapA* single mutant behaved similarly (not shown). These results
8 suggest that ZipA might not be a bundler of FtsZ polymers, contrary to what we initially
9 expected.

10 The region of ZipA known to interact with FtsZ polymers is the FZB (FtsZ Binding)
11 globular domain at its C-terminal end (34, 37, 56, 57). To exclude the possibility that the
12 toxicity of excess ZipA for Δ*zapA*Δ*zapC* cells was due to the accumulation of transmembrane
13 domains at septation sites (49) or because the N-terminal transmembrane region of ZipA
14 might affect cell division by an unknown mechanism, we separated the FZB domain from the
15 transmembrane region. For this purpose we used a chimeric construct containing the C-
16 terminal part of ZipA lacking the transmembrane region ($ZipA_{23-328}$) fused to the N-terminal
17 transmembrane domain of DjlA, ($DjlA_{1-32}$), a protein not related to cell division (37). This
18 hybrid membrane protein containing FZB was cloned into pKG116, a plasmid similar to
19 pKG110 but with a stronger ribosome binding site for increased gene expression. However,
20 similarly to the intact ZipA protein, the $DjlA_{1-32}$-$ZipA_{23-328}$ (FZB) protein was toxic and
21 exacerbated the phenotype of Δ*zapA*Δ*zapC* (Fig. 2E) and Δ*zapA* (not shown) cells. This
22 further suggests that binding of ZipA to FtsZ polymers does not promote their bundling, or at
23 least the type of bundling that could compensate for the lack of ZapA and ZapC (18).
24 To test the model further, we asked whether excess ZipA could rescue the dominant negative
25 effects of an FtsZ allele ($FtsZ_{R174D}$) that was reported to be defective in polymer bundling

bioRxiv preprint doi: https://doi.org/10.1101/319228; this version posted May 14, 2018. The copyright holder for this preprint (which was not certified by peer review) is the author/funder. All rights reserved. No reuse allowed without permission.

1 (14). Although a subsequent study suggested that FtsZR174D was capable of bundling under
2 certain conditions (58), we recently confirmed (Schoenemann et al., in revision) that this
3 protein is indeed more bundling-defective than wild-type FtsZ, as suggested in the original
4 report.

5 To test this idea, we constructed a strain with two plasmids: pDSW210F-ZipA-GFP,
6 and either pKG110-FtsZ or pKG110-$FtsZ_{R174D}$, such that expression of ZipA-GFP is
7 controlled by IPTG and expression of the FtsZ derivatives is controlled by sodium salicylate.
8 The ZipA-GFP is functional and can complement a *zipA1*(ts) mutant (59). Expression of
9 $FtsZ_{R174D}$ at any level above 1 µM sodium salicylate was strongly dominant negative (Fig.
10 S2), in contrast to FtsZ, which allowed viability even at 2.5 µM (and higher, not shown).
11 Notably, ZipA, whether uninduced or induced with IPTG, was unable to counteract the
12 dominant negative effects of $FtsZ_{R174D}$, consistent with the idea that ZipA does not promote
13 FtsZ bundling (Fig. S2). This is in sharp contrast with hyper-bundled FtsZ*, which is able to
14 suppress the dominant negative effects of $FtsZ_{R174D}$ (Schoenemann et al., in revision).
15 Interestingly, the toxicity of ZipA at IPTG concentrations above 50 µM was antagonized by
16 extra FtsZ. One possible explanation is that increased FtsZ bundling triggered by its higher
17 intracellular levels (Fig. 1C) counteracts the negative effects of excess ZipA (Fig. S2).
18

19 **FtsA* and FtsZ* confer at least 10-fold resistance to excess ZipA**

20 In our recent studies, we demonstrated that FtsZ* has an intrinsic capacity to bundle
21 compared with wild-type FtsZ (27), whereas FtsA* can promote bundling of wild-type FtsZ
22 protofilaments (13). Moreover, both gain of function mutants correct the defective division
23 phenotype of Δ*zapA*Δ*zapC* under-bundling mutants (Fig. 1). If ZipA acts to bundle FtsZ
24 polymers, its excess in an *ftsZ** or *ftsA** background should result in over-bundling and be
25 toxic for the cells by inhibiting cell division, as previously reported (Haeusser et al., 2015).

bioRxiv preprint doi: https://doi.org/10.1101/319228; this version posted May 14, 2018. The copyright holder for this preprint (which was not certified by peer review) is the author/funder. All rights reserved. No reuse allowed without permission.

1 To test this idea, we transformed WM1659 and WM4915, which replace the native
2 chromosomal *ftsA* or *ftsZ* with *ftsA** or *ftsZ** alleles, respectively, with pKG110-ZipA in the
3 WM1074 (MG1655) strain background. We found that ZipA overproduction from the *nahG*
4 promoter was toxic at 5 µM sodium salicylate in the wild-type parent strain, and became
5 more toxic at 10 µM inducer (Fig. 3, row 1). In contrast, the presence of *ftsA** in WM1659
6 conferred full resistance against excess ZipA (Fig. 3, row 3), consistent with the original
7 report (48). The effects of *ftsZ** in WM4915 were more modest, but nonetheless resulted in at
8 least a 10-fold increase in resistance at 5 µM inducer (Fig. 3, row 2). The effects of *ftsA**,
9 *ftsZ** or ZipA levels on viability were not due to changes in FtsZ levels, as these remained
10 unchanged in the various conditions (Fig. S1B). The ability of alleles that promote FtsZ
11 protofilament bundling to antagonize ZipA toxicity instead of exacerbate it is yet another
12 argument against the idea that ZipA is a bundler of FtsZ.
13
14 **Excess ZapA and ZapC only partially suppress the thermosensitivity of *zipA1(ts)***
15 We further explored whether ZipA has any functional overlap with Zap proteins by
16 testing if their overproduction could rescue a thermosensitive *zipA1(ts)* mutant (12). We
17 introduced plasmids expressing *ftsZ** (positive control), *zapA*, *zapC*, *zapD,* or a combination
18 of *zapA* + *zapC*, *zapA* + *zapD*, or *zapC* + *zapD* genes into the *zipA1(ts)* strain WM5337. As
19 expected, FtsZ*, ZapA, ZapC, or ZapD all became toxic when overproduced (Fig. 4A), and
20 only *ftsZ** could fully suppress *zipA1(ts)* at 42˚C (27) (Fig. 4C). This suggests that the FtsZ
21 bundling promoted by Zaps cannot substitute for the absence of functional ZipA.
22 The *zipA1(ts)* strain is also inviable at 37ºC, and some factors can suppress the
23 thermosensitivity of *zipA1* at these lower temperatures, including inactivation of certain
24 amino acid biosynthesis genes (59). This suggests that the ZipA1 protein is partially active at
25 37˚C, although not sufficient to sustain viability. To give the Zap proteins the best chance of

bioRxiv preprint doi: https://doi.org/10.1101/319228; this version posted May 14, 2018. The copyright holder for this preprint (which was not certified by peer review) is the author/funder. All rights reserved. No reuse allowed without permission.

1 suppressing *zipA1*, we tested whether the Zap proteins might be able to partially compensate
2 for a partially defective ZipA at this less stringent temperature. We found that neither ZapD
3 nor ZapA were able to suppress *zipA1* thermosensitivity at 37˚C, but ZapC was (Fig. 4B).
4 We also noticed a weak synergistic effect upon coexpression of both ZapA and ZapC, where
5 there was a limited level of viability even at 42ºC (Fig. 4C). Moreover, *zapA* + *zapC*, *zapA* +
6 *zapD*, or *zapC* + *zapD* pairs also conferred partial suppression of *zipA1* thermosensitivity at
7 37ºC (Fig. 4B). These results indicate that the Zap proteins and ZipA may have weak
8 overlapping roles in FtsZ protofilament bundling, perhaps by enhancing the stability of the
9 proto-ring and its tethering to the membrane and to the nucleoid (60).
10
11 **Low surface density ZipA organizes FtsZ into circular protofilament structures on lipid**
12 **monolayers**
13 So far, our *in vivo* data presented here are not consistent with the previous data that
14 suggested ZipA is a major enhancer of FtsZ protofilament bundling. This prompted us to test
15 whether ZipA had any effect on FtsZ bundling in an *in vitro* membrane system. For this, we
16 examined the properties of FtsZ polymers on lipid monolayers. To date, this assay has been
17 mainly used to visualize oligomeric structures of FtsZ protofilaments along with their FtsA
18 membrane tethers by electron microscopy (13, 35, 43, 61, 62). Whereas FtsA has a short C-
19 terminal amphipathic helix that acts as a membrane anchor (11, 61, 63), ZipA has a short N-
20 terminal periplasmic region followed by a transmembrane domain (36, 37, 64).
21 Consequently, full-length ZipA could not be used in our assay.
22 Therefore, we decided to use an N-terminally truncated ZipA (soluble ZipA, sZipA)
23 replacing the first 25 amino acids with an N-terminal His_6 tag (65). To attach sZipA to the
24 lipid monolayer, input lipids were supplemented with a nickel-chelating lipid (DGS-NTA)
25 that anchors the His_6 tag, thus mimicking the membrane topology of the full-length protein

bioRxiv preprint doi: https://doi.org/10.1101/319228; this version posted May 14, 2018. The copyright holder for this preprint (which was not certified by peer review) is the author/funder. All rights reserved. No reuse allowed without permission.

1 (44, 49, 65). The density of sZipA on the lipid monolayer surface was tuned by controlling
2 the amount of NTA lipids added, as these two values are linearly proportional (Sobrinos-
3 Sanguino, Ritcher and Rivas, in preparation). Importantly, we lowered the surface density of
4 ZipA compared with previous studies (39, 44) by using 0.5-1% of NTA lipids instead of
5 10%, which more closely mimic physiologically relevant levels of ZipA. 0.5% NTA
6 corresponds to a surface density of ~2000 ZipA molecules per μm^2. Unperturbed *E. coli* cells
7 contain ~1500 ZipA molecules per cell (66), which corresponds to around 400 molecules per
8 μm^2 assuming a uniform distribution. If 30% of these ZipA molecules are in a midcell ring
9 that comprises 5-10% of the cell length, the estimated protein concentration in the ring would
10 be ~2000 molecules per μm^2, which is the low surface density we used.
11 As expected, when FtsZ was added without sZipA and examined by negative stain
12 transmission EM, FtsZ polymers were scattered sparsely on the lipid monolayer, consistent
13 with the requirement for a membrane anchor such as FtsA or ZipA (1). This residual binding
14 was likely a result of random association of the FtsZ from the added solution onto the grid
15 (Fig. S3B). However, when FtsZ was added to monolayers coated with low-density sZipA,
16 we observed extensive FtsZ protofilament patterns. Most notably, these patterns differed
17 depending on the concentration of NTA lipids, which in turn dictated the concentration of
18 ZipA on the monolayer. For example, when FtsZ (1-5 µM) was polymerized with non-
19 hydrolyzable GTP (GMPcPP) on monolayers seeded with low-density ZipA (0.5% NTA
20 lipids out of the total input lipids), it became strikingly organized into circular structures of
21 mostly single protofilaments in a repetitive pattern (Fig. 5A). These circular structures had an
22 average of nine filaments per polymer. The external diameter was 279 ± 50 nm, with a
23 lumen, lacking filaments, of ~100 nm in diameter. The lateral separation between the
24 filaments was 10 ± 4 nm. The filaments that were closest together mostly appeared as double
25 filaments, but were very loose and non-continuous (more than 70 structures were measured).

bioRxiv preprint doi: https://doi.org/10.1101/319228; this version posted May 14, 2018. The copyright holder for this preprint (which was not certified by peer review) is the author/funder. All rights reserved. No reuse allowed without permission.

1 In the presence of GTP, which should support GTPase activity and filament
2 treadmilling, the ring-like structures contained a smaller number of filaments (6 ± 2) but were
3 larger than the structures formed in GMPcPP, with an external diameter of 400 ± 80 nm and a
4 lumen 190 ± 20 nm in diameter. The GTP-FtsZ filaments appeared more separated than those
5 formed with GMPcPP, as the average separation was 20 ± 9 nm (more than 50 structures
6 were measured) (Fig. 5B). For both GTP and GMPcPP ring-like structures, the spacing
7 measurements were compatible with the FtsZ filament arrangement found in the presence of
8 FtsA minirings (13). To assess the effect of different lipids on these structures, we made lipid
9 monolayers with DOPC. Similar ring-like structures containing FtsZ were observed with
10 GTP (Fig. S4).
11 Next, we asked whether increasing surface density of sZipA might affect the ring-like
12 structures of FtsZ polymers. We saw no difference between monolayers containing 0.5% vs.
13 1% NTA lipids (not shown). We then significantly increased the surface concentration of
14 sZipA on monolayers by increasing the NTA concentration to 10%, mimicking ZipA
15 overproduction *in vivo*. Whereas no oligomeric structures were detectable with sZipA alone
16 (Fig. S3A), when FtsZ was added to the sZipA at this high surface density, polymers were
17 strikingly aligned into parallel tracks of long, straight protofilaments spaced ~20 nm apart,
18 and the formation of ring-like swirls observed at lower ZipA densities was abolished. Even at
19 this high density of ZipA, most of FtsZ protofilaments remained unbundled (Fig. 5C).
20 Whether FtsZ formed straight alignments or swirls was independent of FtsZ concentrations
21 added to the reactions within the 1.5-5 µM physiological range (Fig. 5 and data not shown)
22 (66).
23
24 **FtsZ swirls formed at low ZipA densities are highly dynamic and driven by GTP**
25 **hydrolysis**

bioRxiv preprint doi: https://doi.org/10.1101/319228; this version posted May 14, 2018. The copyright holder for this preprint (which was not certified by peer review) is the author/funder. All rights reserved. No reuse allowed without permission.

1 The ring-like structures formed by FtsZ polymers on low density sZipA resembled the
2 dynamic vortices formed either by FtsZ bound to membrane-attached FtsA or FtsZ fused to
3 YFP and a membrane targeting sequence (FtsZ-YFP-mts) on supported lipid bilayers (44,
4 45). This prompted us to analyze the dynamics of fluorescently labeled FtsZ protofilaments
5 on bilayers containing 0.5% NTA (low density sZipA) using confocal microscopy. When
6 GTP was added to trigger FtsZ polymerization, we observed swirling vortices with a chiral
7 clockwise rotation, similar to those from the aforementioned reports (Fig. 6A, Video S1). A
8 consistently negative slope of the kymographs (Fig. S5) confirmed the directionality of the
9 rotation within the rings. The estimated rotational speed within these structures was ~ 1.8 µm
10 min^{-1}. Similar, but markedly less dynamic swirling rings were observed in the presence of
11 GMPcPP (Fig. 6B, Video S2). The estimated speed was 0.3 µm min^{-1}, consistent with the
12 idea that vortex formation is driven by GTP hydrolysis (45).
13 To visualize the structure of these vortices in more detail, we used super-resolution
14 microscopy (STED). These structures were sharper than those imaged by standard confocal
15 microscopy and their size was similar to the size of the lipid monolayer-attached swirls
16 observed previously by electron microscopy (Fig. 6C). We also used total internal reflection
17 fluorescence microscopy (TIRFM) to visualize the FtsZ swirls at low ZipA surface density.
18 We confirmed that these swirls formed both in GTP and GMPcPP (data not shown).
19 However, the TIRFM approach, which is highly sensitive to the distance of the fluorophore
20 from the surface, was hampered by significant image fluctuation, most probably due to the
21 movement of the unstructured domain of ZipA. This precluded a more precise analysis of the
22 FtsZ swirls by TIRFM.
23
24
25

bioRxiv preprint doi: https://doi.org/10.1101/319228; this version posted May 14, 2018. The copyright holder for this preprint (which was not certified by peer review) is the author/funder. All rights reserved. No reuse allowed without permission.

1 **DISCUSSION**

2 Here, we provide *in vivo* and *in vitro* evidence that ZipA does not inhibit FtsZ
3 treadmilling dynamics, unlike what was suggested previously (44). Instead, when FtsZ
4 protofilaments are tethered to lipids by sZipA at levels that probably more closely mimic
5 physiological conditions, they align and curve to form dynamic swirls that are very similar to
6 those observed previously by FtsA-mediated tethering to lipids (44), direct adsorption to a
7 mica surface (67, 68), or when subjected to crowding agents (69). These swirls, whose
8 dynamics depend on GTP hydrolysis, likely represent treadmilling FtsZ polymers that
9 comprise the FtsZ ring *in vivo* (8, 9). When we tested sZipA at an artificially high density on
10 the lipid surface by applying a high (10%) concentration of NTA lipids, FtsZ protofilaments
11 aligned into large, straight, apparently static structures that are micrometers in length. This
12 observation is consistent with a previous study using high surface concentrations of sZipA,
13 which concluded that ZipA curtails FtsZ dynamics (44). Therefore, we propose that lower
14 surface ZipA densities are necessary to allow FtsZ protofilaments the needed flexibility for
15 their characteristic dynamic movement along the membrane, which is crucial for guiding
16 septum synthesis (8, 9).

17 Despite previous reports that ZipA bundles FtsZ when in solution, including
18 stabilizing highly curved or circular forms of FtsZ polymers (40), here we present several
19 lines of evidence that ZipA does not directly bundle FtsZ protofilaments at lower, probably
20 more physiological densities on lipid surfaces or in *E. coli* cells. When attached to a lipid
21 monolayer at these densities, sZipA efficiently tethers and aligns FtsZ protofilaments, but
22 close lateral associations were uncommon. Even at high surface densities of sZipA that
23 promoted extensive and relatively static FtsZ filament alignments, most protofilaments
24 remain apart, indicating that ZipA does not directly bundle FtsZ like FtsA* does (13).

bioRxiv preprint doi: https://doi.org/10.1101/319228; this version posted May 14, 2018. The copyright holder for this preprint (which was not certified by peer review) is the author/funder. All rights reserved. No reuse allowed without permission.

1 Furthermore, if ZipA actually stimulates FtsZ protofilament bundling, then it might be
2 expected to replace the bundling functions of Zap proteins in cells. Instead, and in contrast to
3 FtsA*, excess ZipA failed to rescue the cell division deficiency of Δ*zapA* or Δ*zapA*Δ*zapC*
4 mutant cells. ZipA also failed to counteract the dominant negative phenotype of the likely
5 bundling-defective $FtsZ_{R174D}$. In another test of ZipA's bundling ability *in vivo*, it was
6 predicted that excess ZipA might be more toxic in a bundling-proficient *ftsA** or *ftsZ** strain
7 background compared with a normal background, due to FtsZ over-bundling. Instead, the
8 *ftsA** or *ftsZ** alleles actually antagonized the toxicity of excess ZipA by at least 10-fold,
9 suggesting again that ZipA is not acting significantly to bundle FtsZ. However, it is also
10 possible that FtsA* and FtsZ* may have already maximally bundled the FtsZ in the cell,
11 leaving no room for additional bundling by ZipA if it were to occur. The mechanism by
12 which *ftsA** or *ftsZ** suppresses ZipA toxicity cannot yet be ascertained, as it is not yet
13 known why excess ZipA is toxic.
14 These results suggest that ZipA is not a significant bundling factor for FtsZ, or at least
15 that its mechanism of action is distinct from that of Zaps, FtsA* and FtsZ*. Nevertheless,
16 extra ZapC could rescue the thermosensitivity of a *zipA1* mutant at 37˚C, and even at the
17 most stringent temperature of 42˚C, a combination of ZapA and ZapC was able to rescue
18 growth somewhat. One explanation for this is that crosslinking of FtsZ polymers by extra
19 ZapA/ZapC generally promotes FtsZ protofilament alignment in parallel superstructures (i.e.,
20 swirls) that mimic the swirls assembled by ZipA, thus stabilizing the proto-ring. Because it is
21 not clear what functions of the mutant ZipA1 protein are compromised at less stringent
22 nonpermissive temperatures, it is difficult to know what ZapC is rescuing at 37˚C that it
23 cannot rescue at 42˚C.
24 This brings up a broader question: why is ZipA essential for divisome function if it
25 performs what seems to be a very similar function as FtsA? Both promote FtsZ protofilament

bioRxiv preprint doi: https://doi.org/10.1101/319228; this version posted May 14, 2018. The copyright holder for this preprint (which was not certified by peer review) is the author/funder. All rights reserved. No reuse allowed without permission.

1 alignment without permitting bundling *in vitro*, and their *in vivo* phenotypes are consistent
2 with this, so why are both necessary *in vivo*? For example, when ZipA is inactivated, even in
3 the presence of FtsA, recruitment of downstream divisome proteins is blocked, implicating
4 ZipA in that essential function (70). We favor the idea that ZipA has additional roles in later
5 divisome function that are distinct from those of FtsA. Furthermore, the ability of certain
6 mutants such as FtsA* and FtsZ* to bypass ZipA may not be due solely to restoration of FtsZ
7 bundling. For example, FtsA* likely recruits downstream divisome proteins more effectively
8 than FtsA, and can accelerate cell division (28, 51, 71). It remains to be seen what these
9 other activities of ZipA are and how they differ from the activities of FtsA. It was previously
10 suggested that the ability of ZipA to form homodimers via its N-terminal domain might
11 enhance FtsZ protofilament bundling (72). Although our lipid monolayer assays probably did
12 not permit homodimerization of sZipA given that the native N terminus is missing, our
13 genetic data using native ZipA suggest that its homodimerization does not significantly
14 promote FtsZ bundling in vivo.

15 Another important question is how the FtsZ protofilaments become aligned as they
16 self-assemble on lipids along with their membrane tethers. The study of plant microtubules
17 may provide clues. During growth of the cortical microtubule array in plant cells,
18 microtubules align with each other in a self-reinforcing mechanism. When a plus end of a
19 microtubule meets another microtubule at an angle of less than 40˚, the first polymer's plus
20 end changes direction and ends up parallel with the encountered polymer. When faced with
21 another microtubule at angles greater than 40˚, the plus end is more likely to disassemble
22 (catastrophe), thus selecting against crossovers and reinforcing parallel alignments (73, 74).
23 Such behavior, coupled with the tendency of intrinsically curved FtsZ protofilaments to adopt
24 the intermediate curved conformation (67, 75, 76), could explain how the swirls become
25 established and self-perpetuate. These curved groups of FtsZ polymers may be important to

bioRxiv preprint doi: https://doi.org/10.1101/319228; this version posted May 14, 2018. The copyright holder for this preprint (which was not certified by peer review) is the author/funder. All rights reserved. No reuse allowed without permission.

1 generate bending forces at the membrane (42, 75). It is possible that highly curved FtsZ also
2 has a role in this activity, given that FtsZ minirings only ~25 nm in diameter can assemble on
3 lipid monolayers (40). Although a specific type of membrane tether is not required for the
4 generation of swirls (45), our data from this study and from our recent report (13) indicate
5 that both FtsA and ZipA maintain FtsZ protofilaments in an aligned but mostly unbundled
6 state. Yet the gain-of-function properties of FtsA* and FtsZ*, and their ability to specifically
7 promote FtsZ lateral interactions, suggest that progression of the divisome requires a set of
8 factors that ultimately switch FtsZ protofilaments to a bundled form. The ability of FtsA* and
9 FtsZ* to bypass ZipA suggests that ZipA itself may be one of these factors, but that it does
10 not necessarily act directly on FtsZ.
11
12 **MATERIALS AND METHODS**
13 **Reagents**
14 *E. coli* polar lipid extract (EcL), 1,2-dioleoyl-*sn*-glycero-3-phosphocholine (DOPC), and 1,2-
15 dioleoyl-sn-glycero-3-[(N-(5-amino-1-carboxypentyl)iminodiacetic acid) succinyl] (nickel
16 salt))(NTA) from Avanti Polar Lipids, Inc. (Alabaster, AL), were kept as 10–20 g/l stocks in
17 chloroform solutions. Alexa Fluor 488 and Alexa Fluor 647 succinimidyl ester were from
18 Molecular Probes/Invitrogen. GTP was from Sigma. GMPcPP (Guanosine-5'-[(α,β)-
19 methyleno]triphosphate, Sodium salt) was from Jena Bioscience. All reactants and salts were
20 of analytical grade (Merck). Chloroform was spectroscopic grade (Merck).
21
22 **Strains, plasmids and cell culture**
23 All *E. coli* strains and plasmid used in this study are listed in Table 1. Cells were grown in
24 Luria-Bertani (LB) medium at 30ºC, 37ºC or 42ºC (as indicated) supplemented with the
25 appropriate antibiotics (ampicillin 50 μg ml^{-1}, chloramphenicol 15 μg ml^{-1} or tetracycline 10

bioRxiv preprint doi: https://doi.org/10.1101/319228; this version posted May 14, 2018. The copyright holder for this preprint (which was not certified by peer review) is the author/funder. All rights reserved. No reuse allowed without permission.

1 μg ml^{-1}) and gene expression inducers, IPTG (Isopropyl beta-D-1-thiogalactopyranoside) and
2 sodium salicylate.
3 Overnight cell cultures were diluted 1:100 in the appropriate media and grown until
4 OD_{600}=0.2 followed by their back-dilution 1:4. After the second dilution, cells were cultured
5 to OD_{600}=0.2 and spotted on plates at 1x, 0.1x, 0.01x, 0.001x, and 0.0001x dilutions from
6 right to left. For DIC microscopy they were further cultured in the presence of inducers,
7 maintained in exponential phase, harvested 2h after induction and fixed with 1%
8 formaldehyde.
9
10 **Plasmid constructions and DNA manipulation**
11 Standard protocols for molecular cloning, transformation, and DNA analysis were used in
12 this study (77). For cloning of $DjlA_{1-32}$-$ZipA_{23-328}$ in salicylate-inducible vector pKG116, we
13 used the *djlA* forward primer (MK17: 5´-
14 GGACTAGTATGCAGTATTGGGGAAAAATCATTGGC-3´) and *zipA* reverse primer
15 (MK18: 5´-AAGGATCCTCAGGCGTTGGCGTCTTT-3´), using pCH172 plasmid (37)
16 kindly provided by Piet de Boer, as template. The cloning was confirmed by DNA
17 sequencing.
18
19 **Protein purification and labeling**
20 *E. coli* FtsZ was purified by the Ca^{2+}-induced precipitation method (78). The soluble mutant
21 of ZipA lacking the trans-membrane region (sZipA) was isolated as described (65). FtsZ and
22 ZipA were labeled with Alexa probes (1:10 molar ratio). FtsZ was labeled under conditions
23 that promote protein polymerization to ensure minimal interference of the dye with FtsZ
24 assembly as described (79).
25

bioRxiv preprint doi: https://doi.org/10.1101/319228; this version posted May 14, 2018. The copyright holder for this preprint (which was not certified by peer review) is the author/funder. All rights reserved. No reuse allowed without permission.

1 **Lipid monolayer assay**

2 Lipid monolayers were prepared as described previously (13, 61). Briefly, 0.2 µg of *E. coli*
3 polar lipid extract supplemented with 0.5-10% of NTA lipids when needed, were floated on
4 Z-buffer (50 mM Tris HCl, pH 7.5, 300 mM KCl, 5 mM $MgCl_2$) using a custom made teflon
5 block (80) and placed in a humid chamber for 1h to evaporate the chloroform. Electron
6 microscopy grids were then placed on the top of each well followed by sequential additions
7 and incubations of 1 µM sZipA (1 h), 0.5-5 µM FtsZ (15 min) and 2 mM GTP or 0.5 mM
8 GMPcPP (5 min). The grids were then removed followed by negative staining with uranyl
9 acetate as described (27) and imaged with a JEOL 1230 electron microscope operated at 100
10 kV coupled with a TVIPS TemCam-F416 CMOS camera. FtsZ protofilament spacing was
11 measured using the Plot Profile tool in ImageJ (81).

12

13 **Self-organization assays on supported lipid bilayers (SLBs)**

14 Lipid bilayers were formed by fusion of small unilamellar vesicles (SUVs) mediated by
15 $CaCl_2$ (82). Lipids (polar extract phospholipids from *E. coli* or DOPC) with or without NTA
16 at 0.5-1% w/w ratios, were prepared by drying a proper amount of the lipid stock solution
17 under a nitrogen stream and kept under vacuum for at least 2 h to remove organic solvent
18 traces. The dried lipid film was dissolved in SLB buffer (50 mM Tris-HCl, pH 7.5, 150 mM
19 KCl) to a final 4 g/l concentration resulting in a solution containing multilamellar vesicles
20 (MLVs). After 10 min sonication of MLVs, small unilamellar vesicles (SUVs) were obtained.
21 One mg/mL suspension of SUVs was added to a hand-operated chamber (a plastic ring
22 attached on a clean glass coverslip using UV-curable glue (Norland Optical Adhesive 63).
23 SLBs were obtained by addition of 2 mM $CaCl_2$ and incubated at 37ºC for 20 min. Samples
24 were washed with pre-warmed SLB buffer to remove non-fused vesicles.

bioRxiv preprint doi: https://doi.org/10.1101/319228; this version posted May 14, 2018. The copyright holder for this preprint (which was not certified by peer review) is the author/funder. All rights reserved. No reuse allowed without permission.

1 Confocal images were collected with a Leica TCS SP5 AOBS inverted confocal
2 microscope with a 63× (N.A. = 1,4–0,6/Oil HCX PL APO, Lbd.Bl.) immersion objective and
3 Confocal multispectral Leica TCS SP8 system with a 3X STED (Stimulation Emission
4 Depletion) module for super-resolution (Leica, Mannheim, Germany). TIRFM experiments
5 were performed on a Leica DMi8 S widefield epifluorescence microscope. Images were
6 acquired every 0.3 s with Hamamatsu Flash 4 sCMOS digital camera.

7 For self-organization assays, SLB buffer was replaced by Z-buffer prior to protein
8 addition. The final volume of the assays was 100 µl. First, 0.5 µM of Alexa Fluor 647-
9 labeled sZipA was added on top of the lipid bilayer with a given amount of NTA lipids. Once
10 the fluorescent sZipA was visualized as attached to the lipid bilayer, 1 µM FtsZ-Alexa 488
11 was added followed by addition of 2 mM GTP (or 0.5 mM of GMPcPP) to induce FtsZ
12 polymerization.

13

14 **Data availability**

15 The authors declare that all data supporting the findings of this study are available within the
16 article, Supplementary Information, or from the authors upon request.

17

18 **Acknowledgements**

19 We thank Sameer Rajesh and Naga Babu Chinnam for strain constructions and preliminary
20 experiments, Miguel Vicente and Ana Isabel Rico for the pJF119HE-FtsZ plasmid and Piet
21 de Boer for the DjlA-ZipA fusion plasmid. We are grateful to members of the Margolin and
22 Rivas laboratories for helpful discussions, and the Confocal Microscopy service at the Centro
23 Nacional de Biotecnología, and the Electron Microscopy and the Confocal Microscopy
24 services at the Centro de Investigaciones Biológicas, both at Consejo Superior de
25 Investigaciones Científicas, for technical support. This work was supported by grant

bioRxiv preprint doi: https://doi.org/10.1101/319228; this version posted May 14, 2018. The copyright holder for this preprint (which was not certified by peer review) is the author/funder. All rights reserved. No reuse allowed without permission.

1 GM61074 from the National Institutes of Health to W.M. and by grant BFU2016-75471-C2-
2 1-P from the Spanish Government to G.R.
3

bioRxiv preprint doi: https://doi.org/10.1101/319228; this version posted May 14, 2018. The copyright holder for this preprint (which was not certified by peer review) is the author/funder. All rights reserved. No reuse allowed without permission.

REFERENCES

1. Krupka M, Margolin W. 2018. Unite to divide: Oligomerization of tubulin and actin homologs regulates initiation of bacterial cell division. F1000Research 7:235.

2. Rico AI, Krupka M, Vicente M. 2013. In the beginning, Escherichia coli assembled the proto-ring: an initial phase of division. J Biol Chem 288:20830–6.

3. Mukherjee A, Lutkenhaus J. 1994. Guanine nucleotide-dependent assembly of FtsZ into filaments. J Bacteriol 176:2754–2758.

4. Bramhill D, Thompson CM. 1994. GTP-dependent polymerization of *Escherichia coli* FtsZ protein to form tubules. Proc Natl Acad Sci USA 91:5813–5817.

5. Erickson HP, Anderson DE, Osawa M. 2010. FtsZ in bacterial cytokinesis: cytoskeleton and force generator all in one. Microbiol Mol Biol Rev 74:504–28.

6. Coltharp C, Xiao J. 2017. Beyond force generation: Why is a dynamic ring of FtsZ polymers essential for bacterial cytokinesis? BioEssays News Rev Mol Cell Dev Biol 39:1–11.

7. Sanchez-Gorostiaga A, Palacios P, Martinez-Arteaga R, Sanchez M, Casanova M, Vicente M. 2016. Life without division: Physiology of *Escherichia coli* FtsZ-deprived filaments. mBio 7:e01620-16.

8. Bisson-Filho AW, Hsu Y-P, Squyres GR, Kuru E, Wu F, Jukes C, Sun Y, Dekker C, Holden S, VanNieuwenhze MS, Brun YV, Garner EC. 2017. Treadmilling by FtsZ filaments drives peptidoglycan synthesis and bacterial cell division. Science 355:739–743.

bioRxiv preprint doi: https://doi.org/10.1101/319228; this version posted May 14, 2018. The copyright holder for this preprint (which was not certified by peer review) is the author/funder. All rights reserved. No reuse allowed without permission.

1 9. Yang X, Lyu Z, Miguel A, McQuillen R, Huang KC, Xiao J. 2017. GTPase activity-
2 coupled treadmilling of the bacterial tubulin FtsZ organizes septal cell wall synthesis.
3 Science 355:744–747.

4 10. Margolin W. 2000. Themes and variations in prokaryotic cell division. FEMS Microbiol
5 Rev 24:531–548.

6 11. Pichoff S, Lutkenhaus J. 2005. Tethering the Z ring to the membrane through a
7 conserved membrane targeting sequence in FtsA. Mol Microbiol 55:1722–1734.

8 12. Pichoff S, Lutkenhaus J. 2002. Unique and overlapping roles for ZipA and FtsA in
9 septal ring assembly in *Escherichia coli*. EMBO J 21:685–693.

10 13. Krupka M, Rowlett VW, Morado DR, Vitrac H, Schoenemann KM, Liu J, Margolin W.
11 2017. *Escherichia coli* FtsA forms lipid-bound minirings that antagonize lateral
12 interactions between FtsZ protofilaments. Nat Commun 8:15957.

13 14. Koppelman CM, Aarsman ME, Postmus J, Pas E, Muijsers AO, Scheffers DJ, Nanninga
14 N, den Blaauwen T. 2004. R174 of *Escherichia coli* FtsZ is involved in membrane
15 interaction and protofilament bundling, and is essential for cell division. Mol Microbiol
16 51:645–57.

17 15. Shin JY, Vollmer W, Lagos R, Monasterio O. 2013. Glutamate 83 and arginine 85 of
18 helix H3 bend are key residues for FtsZ polymerization, GTPase activity and cellular
19 viability of *Escherichia coli*: lateral mutations affect FtsZ polymerization and E. coli
20 viability. BMC Microbiol 13:26.

bioRxiv preprint doi: https://doi.org/10.1101/319228; this version posted May 14, 2018. The copyright holder for this preprint (which was not certified by peer review) is the author/funder. All rights reserved. No reuse allowed without permission.

1 16. Marquez IF, Mateos-Gil P, Shin JY, Lagos R, Monasterio O, Velez M. 2017. Mutations
2 on FtsZ lateral helix H3 that disrupt cell viability hamper reorganization of polymers on
3 lipid surfaces. Biochim Biophys Acta 1859:1815–1827.

4 17. Dajkovic A, Pichoff S, Lutkenhaus J, Wirtz D. 2010. Cross-linking FtsZ polymers into
5 coherent Z rings. Mol Microbiol 78:651–68.

6 18. Huang KH, Durand-Heredia J, Janakiraman A. 2013. FtsZ ring stability: of bundles,
7 tubules, crosslinks, and curves. J Bacteriol 195:1859–1868.

8 19. Gueiros-Filho FJ, Losick R. 2002. A widely conserved bacterial cell division protein
9 that promotes assembly of the tubulin-like protein FtsZ. Genes Dev 16:2544–2556.

10 20. Durand-Heredia J, Rivkin E, Fan G, Morales J, Janakiraman A. 2012. Identification of
11 ZapD as a cell division factor that promotes the assembly of FtsZ in *Escherichia coli*. J
12 Bacteriol 194:3189–98.

13 21. Durand-Heredia JM, Yu HH, De Carlo S, Lesser CF, Janakiraman A. 2011.
14 Identification and characterization of ZapC, a stabilizer of the FtsZ ring in *Escherichia*
15 *coli*. J Bacteriol 193:1405–13.

16 22. Hale CA, Shiomi D, Liu B, Bernhardt TG, Margolin W, Niki H, de Boer PA. 2011.
17 Identification of *Escherichia coli* ZapC (YcbW) as a component of the division
18 apparatus that binds and bundles FtsZ polymers. J Bacteriol 193:1393–404.

19 23. Galli E, Gerdes K. 2010. Spatial resolution of two bacterial cell division proteins: ZapA
20 recruits ZapB to the inner face of the Z-ring. Mol Microbiol 76:1514–26.

21 24. Stricker J, Erickson HP. 2003. In vivo characterization of *Escherichia coli* ftsZ mutants:
22 effects on Z-ring structure and function. J Bacteriol 185:4796–805.

bioRxiv preprint doi: https://doi.org/10.1101/319228; this version posted May 14, 2018. The copyright holder for this preprint (which was not certified by peer review) is the author/funder. All rights reserved. No reuse allowed without permission.

1 25. Jaiswal R, Patel RY, Asthana J, Jindal B, Balaji PV, Panda D. 2010. E93R substitution
2 of *Escherichia coli* FtsZ induces bundling of protofilaments, reduces GTPase activity,
3 and impairs bacterial cytokinesis. J Biol Chem 285:31796–805.

4 26. Encinar M, Kralicek AV, Martos A, Krupka M, Cid S, Alonso A, Rico AI, Jimenez M,
5 Velez M. 2013. Polymorphism of FtsZ filaments on lipid surfaces: role of monomer
6 orientation. Langmuir 29:9436–46.

7 27. Haeusser DP, Rowlett VW, Margolin W. 2015. A mutation in *Escherichia coli* ftsZ
8 bypasses the requirement for the essential division gene zipA and confers resistance to
9 FtsZ assembly inhibitors by stabilizing protofilament bundling. Mol Microbiol 97:988–
10 1005.

11 28. Pichoff S, Shen B, Sullivan B, Lutkenhaus J. 2012. FtsA mutants impaired for self-
12 interaction bypass ZipA suggesting a model in which FtsA's self-interaction competes
13 with its ability to recruit downstream division proteins. Mol Microbiol 83:151–67.

14 29. Hernandez-Rocamora VM, Reija B, Garcia C, Natale P, Alfonso C, Minton AP, Zorrilla
15 S, Rivas G, Vicente M. 2012. Dynamic interaction of the *Escherichia coli* cell division
16 ZipA and FtsZ proteins evidenced in nanodiscs. J Biol Chem 287:30097–104.

17 30. Hernandez-Rocamora VM, Garcia-Montanes C, Rivas G, Llorca O. 2012.
18 Reconstitution of the *Escherichia coli* cell division ZipA-FtsZ complexes in nanodiscs
19 as revealed by electron microscopy. J Struct Biol 180:531–8.

20 31. Pazos M, Natale P, Vicente M. 2013. A specific role for the ZipA protein in cell
21 division: stabilization of the FtsZ protein. J Biol Chem 288:3219–26.

bioRxiv preprint doi: https://doi.org/10.1101/319228; this version posted May 14, 2018. The copyright holder for this preprint (which was not certified by peer review) is the author/funder. All rights reserved. No reuse allowed without permission.

1 32. Ma X, Margolin W. 1999. Genetic and functional analyses of the conserved C-terminal
2 core domain of *Escherichia coli* FtsZ. J Bacteriol 181:7531–7544.

3 33. Wang X, Huang J, Mukherjee A, Cao C, Lutkenhaus J. 1997. Analysis of the interaction
4 of FtsZ with itself, GTP, and FtsA. J Bacteriol 179:5551–5559.

5 34. Mosyak L, Zhang Y, Glasfeld E, Haney S, Stahl M, Seehra J, Somers WS. 2000. The
6 bacterial cell-division protein ZipA and its interaction with an FtsZ fragment revealed
7 by X-ray crystallography. EMBO J 19:3179–91.

8 35. Szwedziak P, Wang Q, Freund SM, Löwe J. 2012. FtsA forms actin-like protofilaments.
9 EMBO J 31:2249–2260.

10 36. Raychaudhuri D. 1999. ZipA is a MAP-Tau homolog and is essential for structural
11 integrity of the cytokinetic FtsZ ring during bacterial cell division. EMBO J 18:2372–
12 2383.

13 37. Hale CA, Rhee AC, de Boer PA. 2000. ZipA-induced bundling of FtsZ polymers
14 mediated by an interaction between C-terminal domains. J Bacteriol 182:5153–5166.

15 38. Kuchibhatla A, Bhattacharya A, Panda D. 2011. ZipA binds to FtsZ with high affinity
16 and enhances the stability of FtsZ protofilaments. PLoS One 6:e28262.

17 39. Mateos-Gil P, Marquez I, Lopez-Navajas P, Jimenez M, Vicente M, Mingorance J,
18 Rivas G, Velez M. 2012. FtsZ polymers bound to lipid bilayers through ZipA form
19 dynamic two dimensional networks. Biochim Biophys Acta 1818:806–13.

20 40. Chen Y, Huang H, Osawa M, Erickson HP. 2017. ZipA and FtsA* stabilize FtsZ-GDP
21 miniring structures. Sci Rep 7:3650.

bioRxiv preprint doi: https://doi.org/10.1101/319228; this version posted May 14, 2018. The copyright holder for this preprint (which was not certified by peer review) is the author/funder. All rights reserved. No reuse allowed without permission.

1 41. Osawa M, Anderson DE, Erickson HP. 2008. Reconstitution of contractile FtsZ rings in
2 liposomes. Science 320:792–4.

3 42. Osawa M, Erickson HP. 2013. Liposome division by a simple bacterial division
4 machinery. Proc Natl Acad Sci USA 110:11000–11004.

5 43. Szwedziak P, Wang Q, Bharat TAM, Tsim M, Löwe J. 2014. Architecture of the ring
6 formed by the tubulin homologue FtsZ in bacterial cell division. eLife 3:e04601.

7 44. Loose M, Mitchison TJ. 2014. The bacterial cell division proteins FtsA and FtsZ self-
8 organize into dynamic cytoskeletal patterns. Nat Cell Biol 16:38–46.

9 45. Ramirez D, Garcia-Soriano DA, Raso A, Feingold M, Rivas G, Schwille P. 2017. Chiral
10 vortex dynamics on membranes is an intrinsic property of FtsZ, driven by GTP
11 hydrolysis. BioRxiv 79533.

12 46. Sobrinos-Sanguino M, Zorrilla S, Monterroso B, Minton AP, Rivas G. 2017. Nucleotide
13 and receptor density modulate binding of bacterial division FtsZ protein to ZipA
14 containing lipid-coated microbeads. Sci Rep 7:13707.

15 47. Conti J, Viola MG, Camberg JL. 2018. FtsA reshapes membrane architecture and
16 remodels the Z-ring in *Escherichia coli*. Mol Microbiol 107:558–576.

17 48. Geissler B, Elraheb D, Margolin W. 2003. A gain of function mutation in ftsA bypasses
18 the requirement for the essential cell division gene zipA in *Escherichia coli*. Proc Natl
19 Acad Sci USA 100:4197–4202.

20 49. Cabré EJ, Sanchez-Gorostiaga A, Carrara P, Ropero N, Casanova M, Palacios P, Stano
21 P, Jimenez M, Rivas G, Vicente M. 2013. Bacterial division proteins FtsZ and ZipA
22 induce vesicle shrinkage and cell membrane invagination. J Biol Chem 288:26625–34.

bioRxiv preprint doi: https://doi.org/10.1101/319228; this version posted May 14, 2018. The copyright holder for this preprint (which was not certified by peer review) is the author/funder. All rights reserved. No reuse allowed without permission.

1 50. Geissler B, Margolin W. 2005. Evidence for functional overlap among multiple
2 bacterial cell division proteins: compensating for the loss of FtsK. Mol Microbiol
3 58:596–612.

4 51. Geissler B, Shiomi D, Margolin W. 2007. The ftsA* gain-of-function allele of
5 *Escherichia coli* and its effects on the stability and dynamics of the Z ring.
6 Microbiology 153:814–825.

7 52. Ortiz C, Casanova M, Palacios P, Vicente M. 2017. The hypermorph FtsA* protein has
8 an in vivo role in relieving the *Escherichia coli* proto-ring block caused by excess ZapC.
9 PloS One 12:e0184184.

10 53. Samaluru H, SaiSree L, Reddy M. 2007. Role of SufI (FtsP) in cell division of
11 *Escherichia coli*: evidence for its involvement in stabilizing the assembly of the
12 divisome. J Bacteriol 189:8044–8052.

13 54. Haeusser DP, Margolin W. 2016. Splitsville: structural and functional insights into the
14 dynamic bacterial Z ring. Nat Rev Microbiol 14:305–319.

15 55. Bernhardt TG, de Boer PA. 2003. The *Escherichia coli* amidase AmiC is a periplasmic
16 septal ring component exported via the twin-arginine transport pathway. Mol Microbiol
17 48:1171–1182.

18 56. Moy FJ, Glasfeld E, Mosyak L, Powers R. 2000. Solution structure of ZipA, a crucial
19 component of *Escherichia coli* cell division. Biochemistry (Mosc) 39:9146–56.

20 57. Du S, Park K-T, Lutkenhaus J. 2014. Oligomerization of FtsZ converts the FtsZ tail
21 motif (CCTP) into a multivalent ligand with high avidity for partners ZipA and SlmA.
22 Mol Microbiol. 95:173-188.

bioRxiv preprint doi: https://doi.org/10.1101/319228; this version posted May 14, 2018. The copyright holder for this preprint (which was not certified by peer review) is the author/funder. All rights reserved. No reuse allowed without permission.

1 58. Moore DA, Whatley ZN, Joshi CP, Osawa M, Erickson HP. 2017. Probing for binding
2 regions of the FtsZ protein surface through site-directed insertions: Discovery of fully
3 functional FtsZ-fluorescent proteins. J Bacteriol 199:e00553-16.

4 59. Vega DE, Margolin W. 2018. Suppression of a thermosensitive zipA cell division
5 mutant by altering amino acid metabolism. J Bacteriol 200:e00535-17.

6 60. Buss J, Coltharp C, Shtengel G, Yang X, Hess H, Xiao J. 2015. A multi-layered protein
7 network stabilizes the *Escherichia coli* FtsZ-ring and modulates constriction dynamics.
8 PLoS Genet 11:e1005128.

9 61. Krupka M, Cabre EJ, Jimenez M, Rivas G, Rico AI, Vicente M. 2014. Role of the FtsA
10 C terminus as a switch for polymerization and membrane association. mBio 5:e02221.

11 62. Erickson HP, Taylor DW, Taylor KA, Bramhill D. 1996. Bacterial cell division protein
12 FtsZ assembles into protofilament sheets and minirings, structural homologs of tubulin
13 polymers. Proc Natl Acad Sci USA 93:519–523.

14 63. Lowe J, van den Ent F. 2001. Conserved sequence motif at the C-terminus of the
15 bacterial cell- division protein FtsA. Biochimie 83:117–20.

16 64. Hale CA, de Boer PA. 1997. Direct binding of FtsZ to ZipA, an essential component of
17 the septal ring structure that mediates cell division in *E. coli*. Cell 88:175–185.

18 65. Martos A, Alfonso C, Lopez-Navajas P, Ahijado-Guzmn R, Mingorance J, Minton AP,
19 Rivas G. 2010. Characterization of self-association and heteroassociation of bacterial
20 cell division proteins FtsZ and ZipA in solution by composition gradient-static light
21 scattering. Biochemistry (Mosc) 49:10780–10787.

bioRxiv preprint doi: https://doi.org/10.1101/319228; this version posted May 14, 2018. The copyright holder for this preprint (which was not certified by peer review) is the author/funder. All rights reserved. No reuse allowed without permission.

1 66. Rueda S, Vicente M, Mingorance J. 2003. Concentration and assembly of the division
2 ring proteins FtsZ, FtsA, and ZipA during the *Escherichia coli* cell cycle. J Bacteriol
3 185:3344–3351.

4 67. Mingorance J, Tadros M, Vicente M, Gonzalez JM, Rivas G, Velez M. 2005.
5 Visualization of single *Escherichia coli* FtsZ filament dynamics with atomic force
6 microscopy. J Biol Chem 280:20909–20914.

7 68. Mateos-Gil P, Paez A, Horger I, Rivas G, Vicente M, Tarazona P, Velez M. 2012.
8 Depolymerization dynamics of individual filaments of bacterial cytoskeletal protein
9 FtsZ. Proc Natl Acad Sci USA 109:8133–8.

10 69. Popp D, Iwasa M, Narita A, Erickson HP, Maeda Y. 2009. FtsZ condensates: an in vitro
11 electron microscopy study. Biopolymers 91:340–350.

12 70. Hale CA, de Boer PA. 2002. ZipA is required for recruitment of FtsK, FtsQ, FtsL, and
13 FtsN to the septal ring in *Escherichia coli*. J Bacteriol 184:2552–2556.

14 71. Liu B, Persons L, Lee L, DeBoer P. 2015. Roles for both FtsA and the FtsBLQ
15 subcomplex in FtsN-stimulated cell constriction in *Escherichia coli*. Mol Microbiol
16 95:945–970.

17 72. Skoog K, Daley DO. 2012. The *Escherichia coli* cell division protein ZipA forms
18 homodimers prior to association with FtsZ. Biochemistry (Mosc) 51:1407–15.

19 73. Shaw SL, Kamyar R, Ehrhardt DW. 2003. Sustained microtubule treadmilling in
20 Arabidopsis cortical arrays. Science 300:1715–1718.

21 74. Dixit R, Cyr R. 2004. The cortical microtubule array: from dynamics to organization.
22 Plant Cell 16:2546–2552.

bioRxiv preprint doi: https://doi.org/10.1101/319228; this version posted May 14, 2018. The copyright holder for this preprint (which was not certified by peer review) is the author/funder. All rights reserved. No reuse allowed without permission.

1 75. Erickson HP, Osawa M. 2017. FtsZ constriction force - curved protofilaments bending
2 membranes. Subcell Biochem 84:139–160.

3 76. Li Y, Hsin J, Zhao L, Cheng Y, Shang W, Huang KC, Wang HW, Ye S. 2013. FtsZ
4 protofilaments use a hinge-opening mechanism for constrictive force generation.
5 Science 341:392–395.

6 77. Sambrook J, Fritsch EF, Maniatis T. 1989. Molecular Cloning: a Laboratory Manual,
7 2nd ed. Cold Spring Harbor Laboratory Press, Cold Spring Harbor, New York.

8 78. Rivas G, Lopez A, Mingorance J, Ferrandiz MJ, Zorrilla S, Minton AP, Vicente M,
9 Andreu JM. 2000. Magnesium-induced linear self-association of the FtsZ bacterial cell
10 division protein monomer. The primary steps for FtsZ assembly. J Biol Chem
11 275:11740–9.

12 79. Gonzalez JM, Jimenez M, Velez M, Mingorance J, Andreu JM, Vicente M, Rivas G.
13 2003. Essential cell division protein FtsZ assembles into one monomer-thick ribbons
14 under conditions resembling the crowded intracellular environment. J Biol Chem
15 278:37664–37671.

16 80. Sanchez-Gorostiaga, A., Rico AI, P. Natale, Krupka M, Vicente M. 2015. Marrying
17 single molecules to single cells: Protocols for the study of the bacterial proto-ring
18 components essential for division.Hydrocarbon and Lipid Microbiology Protocols.
19 Springer-Verlag, Heidelberg.

20 81. Schneider CA, Rasband WS, Eliceiri KW. 2012. NIH Image to ImageJ: 25 years of
21 image analysis. Nat Methods 9:671–675.

bioRxiv preprint doi: https://doi.org/10.1101/319228; this version posted May 14, 2018. The copyright holder for this preprint (which was not certified by peer review) is the author/funder. All rights reserved. No reuse allowed without permission.

1 82. Martos A, Raso A, Jimenez M, Petrasek Z, Rivas G, Schwille P. 2015. FtsZ polymers
2 tethered to the membrane by ZipA are susceptible to spatial regulation by Min waves.
3 Biophys J 108:2371–2383.

4 83. Miroux B, Walker JE. 1996. Over-production of proteins in *Escherichia coli*: mutant
5 hosts that allow synthesis of some membrane proteins and globular proteins at high
6 levels. J Mol Biol 260:289–98.

7 84. Mowery P, Ames P, Reiser RH, Parkinson JS. 2015. Chemotactic signaling by single-
8 chain chemoreceptors. PloS One 10:e0145267.

9 85. Han X-S, Parkinson JS. 2014. An unorthodox sensory adaptation site in the *Escherichia*
10 *coli* serine chemoreceptor. J Bacteriol 196:641–649.

11 86. Shiomi D, Margolin W. 2007. Dimerization or oligomerization of the actin-like FtsA
12 protein enhances the integrity of the cytokinetic Z ring. Mol Microbiol 66:1396–1415.

13

bioRxiv preprint doi: https://doi.org/10.1101/319228; this version posted May 14, 2018. The copyright holder for this preprint (which was not certified by peer review) is the author/funder. All rights reserved. No reuse allowed without permission.

1 **Figure legends**

2 **Figure 1. FtsA* or excess FtsZ can rescue the FtsZ bundling deficient Δ*zapA*Δ*zapC*
3 mutant.** (A) Cells of the TB28 parent, or (B-D) Δ*zapA*Δ*zapC* double mutant carrying either
4 no plasmid (B), pJF119HE-FtsZ (C) or pDSW210F-FtsA* (D) were grown to mid-
5 logarithmic phase in LB medium (supplemented with 50 μM IPTG in C) and imaged using
6 DIC. Scale bar= 10 μm.

7

8 **Figure 2. Excess ZipA or a ZipA with a swapped transmembrane domain cannot
9 compensate for cell division deficiencies of Δ*zap* mutants.** (A) TB28 and Zap-deletion
10 strains Δ*zapA* and Δ*zapA*Δ*zapC* transformed with pKG110 empty vector (EV) or pKG110-
11 ZipA (pZipA) were grown to exponential phase and plate spotted IN 10-fold dilutions at
12 different concentrations of inducer (sodium salicylate; Na-Sal). (B-E) Representative DIC
13 images of Δ*zapA*Δ*zapC* cells transformed with pKG110-ZipA (B-D) and pKG116-DjlA$_{1-32}$-
14 ZipA$_{23-328}$ (E) are shown (see panel descriptions and text). Scale bar= 10 μm.

15

16 **Figure 3. The *ftsZ** or *ftsA** alleles counteract the toxicity of excess ZipA**. WM1074
17 wild-type strain and its derivatives containing chromosomal *ftsA** (WM1659) and *ftsZ**
18 (WM4915), transformed with pKG110-ZipA were grown to exponential phase and spotted on
19 plates at 10-fold dilutions with different concentrations of inducer (sodium salicylate; Na-
20 Sal).

21

22 **Figure 4. Excess Zap proteins only weakly suppress the *zipA1* thermosensitive allele.**
23 The WM5337 *zipA1* thermosensitive strain was transformed with the pairs of compatible
24 plasmids indicated at each row, and spotted on pre-warmed plates at 10-fold dilutions

bioRxiv preprint doi: https://doi.org/10.1101/319228; this version posted May 14, 2018. The copyright holder for this preprint (which was not certified by peer review) is the author/funder. All rights reserved. No reuse allowed without permission.

1 containing indicated concentrations of inducers (IPTG for pDSW plasmids and Na-Sal for
2 pKG116) and incubated at 30, 37 and 42ºC.
3
4 **Figure 5. Assembly of FtsZ on *E. coli* polar lipid monolayers containing sZipA**
5 **visualized by negative stain transmission electron microscopy.** (A) Examples of circular
6 structures of FtsZ single filaments on a lipid monolayer containing 0.5% DGS-NTA and
7 sZipA (1 µM) in the presence of GMPcPP. FtsZ concentration was 1.5 µM. Scale bar = 200
8 nm. (B) Examples of circular structures of FtsZ single filaments on a sZipA-containing
9 monolayer with 1% of DGS-NTA in the presence of GTP. FtsZ concentration was 2.5 µM.
10 Scale bar = 200 nm. (C) Straight FtsZ filaments assembled in the presence of GTP on a lipid
11 monolayer with a high surface density of sZipA (attached to 10% of DGS-NTA). The
12 arrowhead highlights a typical single protofilament; the full arrow highlights a less common
13 double protofilament. FtsZ and sZipA concentrations were 5 and 2 µM, respectively. Grids
14 for all three panels were negatively stained and visualized by electron microscopy. Scale bar
15 = 100 nm.
16
17 **Figure 6. Fluorescence microscopic images of FtsZ assembly on SLBs of *E. coli* polar**
18 **lipids containing sZipA.** (A) Assembly of Alexa 488-labeled FtsZ into dynamic vortices
19 after GTP addition. (B) Assembly of similar circular structures after GMPcPP addition. (C)
20 Representative high resolution STED image of the experiment shown in panel B. FtsZ and
21 sZipA concentrations were 1 µM. Scale bars = 1 µm.
22
23
24
25

bioRxiv preprint doi: https://doi.org/10.1101/319228; this version posted May 14, 2018. The copyright holder for this preprint (which was not certified by peer review) is the author/funder. All rights reserved. No reuse allowed without permission.

1 **Supplemental Figure legends:**

2

3 **Figure S1. Immunoblots showing cellular levels of FtsZ and ZipA in various induction**
4 **conditions and genotypes.** SDS-PAGE of cell extracts from (A) TB28 (WT), Δ*zapA* (Δ*A*)
5 and Δ*zapA*Δ*zapC* (Δ*AC*) backgrounds and (B) WM1074 (WT) and its derivatives containing
6 chromosomal *ftsA** and *ftsZ** were blotted and probed with anti-FtsZ or anti-ZipA polyclonal
7 antibodies (48). Relative band intensities for each of the 4 blots were analyzed and plotted in
8 ImageJ, with the weakest band in each set normalized to 1.

9

10 **Figure S2. Excess ZipA cannot counteract the dominant negative effects of an under-**
11 **bundled FtsZ.** WM1074 wild-type cells co-transformed with pKG110-FtsZ (p-FtsZ) or
12 toxic, dominant negative $FtsZ_{R174D}$ (p-$FtsZ_{R174D}$) and pDSW210 (pEV) or pDSW210-ZipA-
13 GFP (pZipA) were spotted on plates containing indicated concentrations of inducers to test if
14 the toxicity of $FtsZ_{R174D}$ could be antagonized by ZipA.

15

16 **Figure S3. sZipA does not form structures on lipid monolayers and FtsZ only forms**
17 **residual sporadic filaments on monolayers supplemented with DGS-NTA.** sZipA (2 µM)
18 was incubated on lipid monolayers containing 10% NTA lipids (A). 5 µM FtsZ was
19 incubated on monolayers with 1% of NTA lipids, but not seeded with sZipA (B). Grids were
20 negatively stained and visualized by electron microscopy. Arrow highlights a single FtsZ
21 protofilament. Scale bar= 100 nm.

22

23 **Figure S4. Assembly of FtsZ on lipid monolayers containing sZipA and the effect of**
24 **FtsZ concentration and of lipid composition**. (A) Circular structures of FtsZ single
25 filaments on a DOPC monolayer containing 1% of DGS-NTA and 2 µM sZipA in the

bioRxiv preprint doi: https://doi.org/10.1101/319228; this version posted May 14, 2018. The copyright holder for this preprint (which was not certified by peer review) is the author/funder. All rights reserved. No reuse allowed without permission.

1 presence of GMPcPP. FtsZ concentration was 5 μM. (B) The equivalent experiment was
2 performed on an *E. coli* polar lipid monolayer. Scale bars are shown.
3
4 **Figure S5. Kymographs of FtsZ swirls on SLBs carrying low-density sZipA**.
5 Representative kymographs tracking the circumferential motion of individual FtsZ Alexa 488
6 swirls (as seen on videos) (A) with added GTP or (B) with added GMPcPP. Time and length
7 scales are indicated, and black lines denote two representative paths of traveling fluorescence
8 intensities. The slopes of the lines correspond to the velocity (x/t). Kymographs were
9 obtained using an ImageJ kymograph plugin (Jens Rietdorf and Arne Seitz, EMBL,
10 Heidelberg); 20 different circular structures were analyzed.
11
12 **Video S1: GTP-dependent assembly of FtsZ on supported *E. coli* lipid bilayers**
13 **containing low-density sZipA**. Video of FtsZ ring-like filaments formation after GTP
14 addition. FtsZ Alexa Fluor 488 and sZipA concentrations are the same as in Figure 6A.
15
16 **Video S2: GMPcPP-dependent assembly of FtsZ on supported *E. coli* lipid bilayers**
17 **containing low-density sZipA**. Video of FtsZ ring-like filaments formation after GMPcPP
18 addition. FtsZ Alexa Fluor 488 and sZipA concentrations are the same as in Figure 6B.
19
20
21

bioRxiv preprint doi: https://doi.org/10.1101/319228; this version posted May 14, 2018. The copyright holder for this preprint (which was not certified by peer review) is the author/funder. All rights reserved. No reuse allowed without permission.

1 **Table 1. Strains and plasmids used in this study.**

2

Strain	**Description**	**Source/reference**
BL21/DE3	Host for protein overproduction	(83)
C43	Host for protein overproduction	(83)
TB28	MG1655 Δ*lacIZYA*::*frt*	(55)
TOP10	Cloning strain	Invitrogen
WM1074	MG1655 Δ*lacU169*	Lab collection
WM1659	WM1074 *ftsA** *leuO*::Tn*10*	(48)
WM4842	TB28 Δ*zapA::frt*	(20)
WM4843	TB28 Δ*zapA::frt* Δ*zapC::kan*	(20)
WM4915	WM1074 *ftsZ** *leuO*::Tn*10*	(27)
Plasmid	**Description**	**Source/reference**
pKG110	pACYC184 derivative with *nahG* promoter	(84)
pKG116	pKG110 with stronger ribosome binding site	(85)
pDH156	pKG110-FtsZ	(27)
pDH159	pKG116-FtsZ*	(27)
pWM1851	pDSW207-ZapA	Lab collection
pWM2784	pDSW210-FLAG	(86)
pWM2787	pWM2784-FtsA*	(86)
pWM2978	pDSW208-ZapC	(22)
pWM3073	pKG110-ZipA	(86)
pWM3074	pKG116-ZapA	(86)
pWM4651	pKG110-ZapA	(13)
pWM5265	pDSW210-ZipA-GFP	(59)
pWM5310	pKG116-ZapC	This study
pWM5366	pKG110-$FtsZ_{R174D}$	Kara Schoenemann
pWM5674	pKG116-ZapD	This study
pWM5883	pKG116-$DjlA_{1-32}$-$ZipA_{23-328}$	Sameer Rajesh
pMFV56	pET28a-FtsZ	(78)
pCH172	DjlA-ZipA fusion	(37)
pJF119HE-FtsZ	IPTG-inducible *ftsZ* on plasmid	(26)
pET15-sZip	IPTG-inducible *szipA* on plasmid	(65)

3
4

5

6

7

8

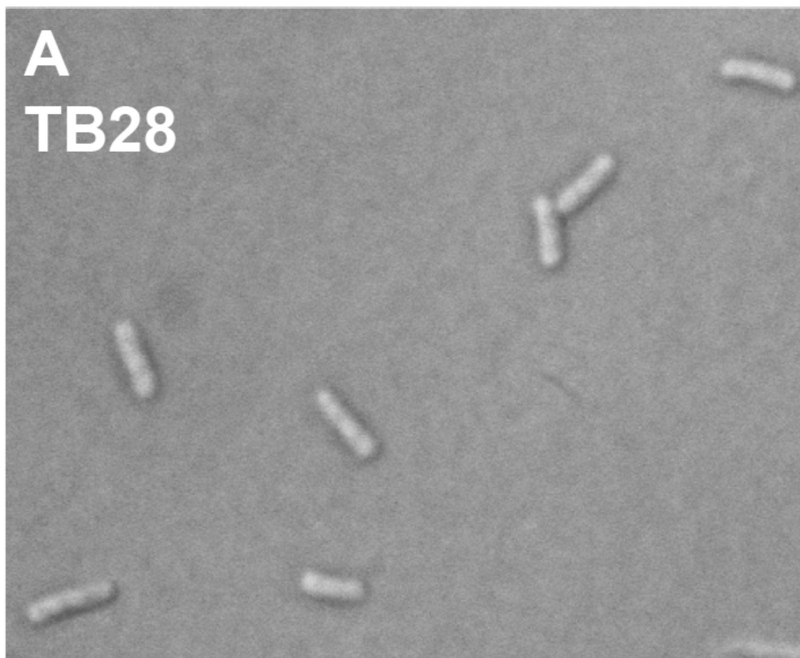
A
TB28

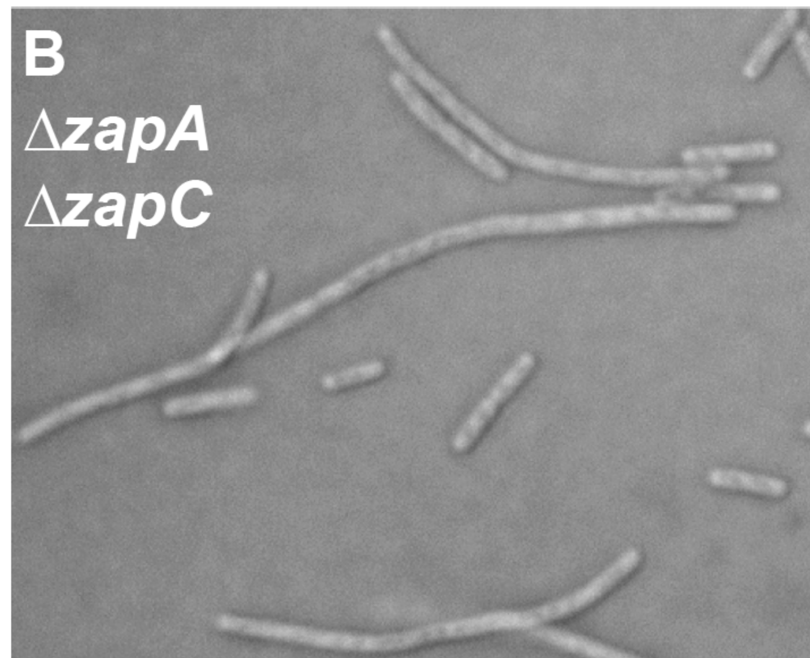
B
ΔzapA
ΔzapC

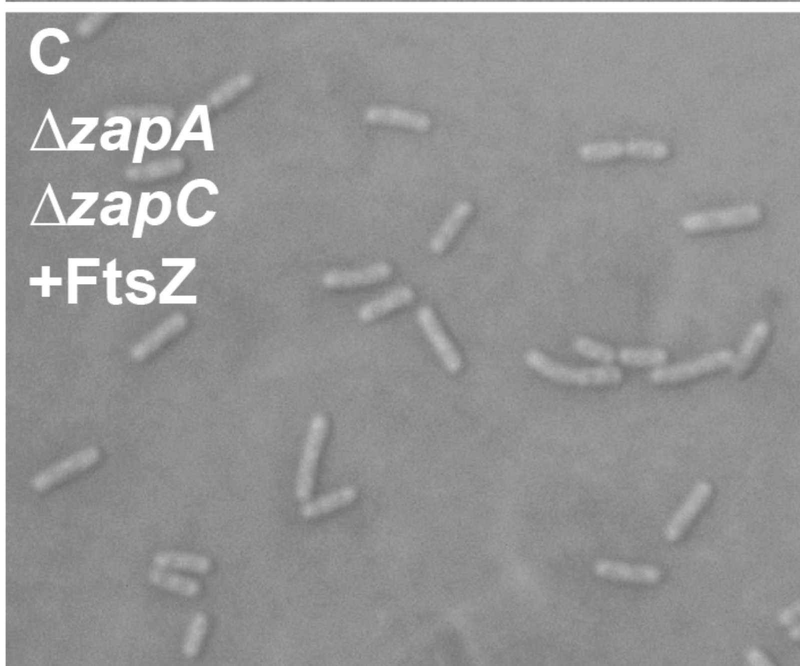
C
ΔzapA
ΔzapC
+FtsZ

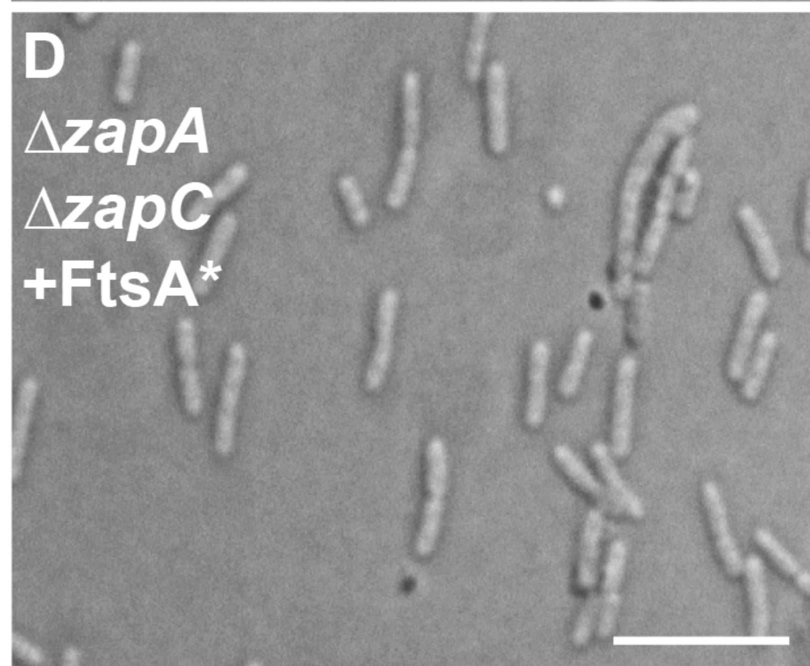
D
ΔzapA
ΔzapC
+FtsA*

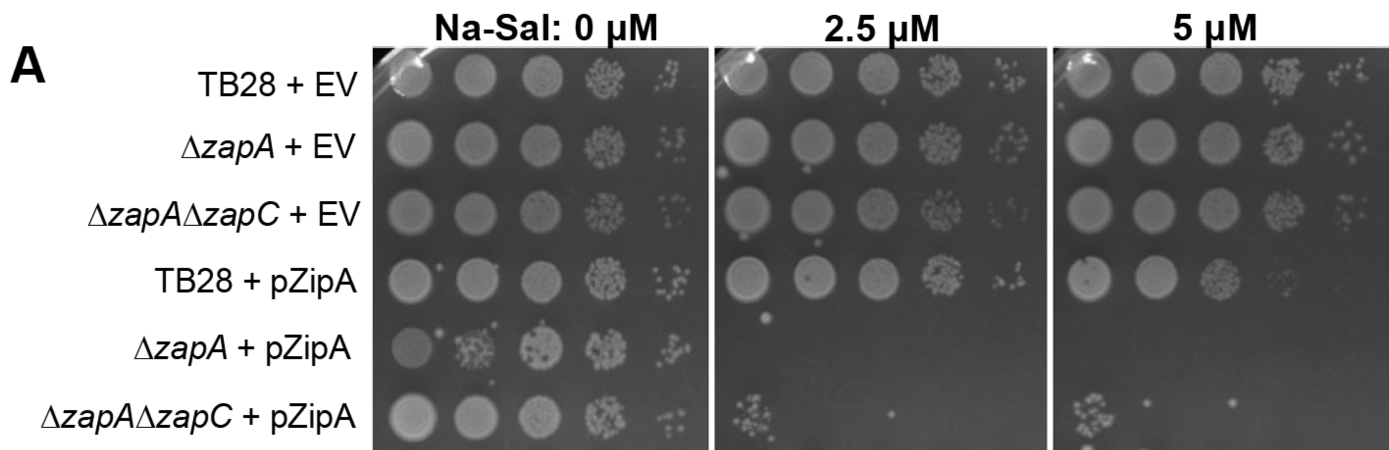

A
Na-Sal: 0 µM
2.5 µM
5 µM
TB28 + EV
ΔzapA + EV
ΔzapAΔzapC + EV
TB28 + pZipA
ΔzapA + pZipA
ΔzapAΔzapC + pZipA

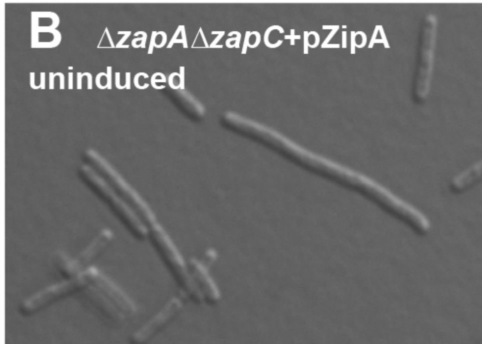

B ΔzapAΔzapC+pZipA
uninduced

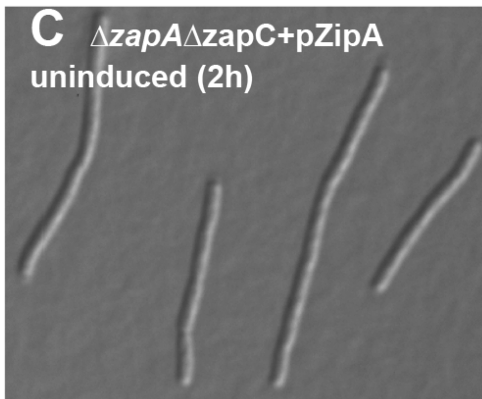

C ΔzapAΔzapC+pZipA
uninduced (2h)

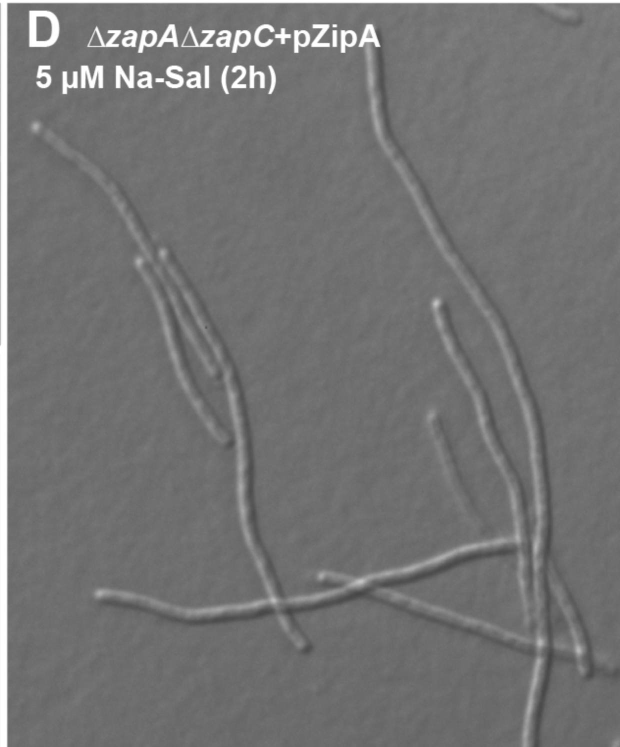

D ΔzapAΔzapC+pZipA
5 µM Na-Sal (2h)

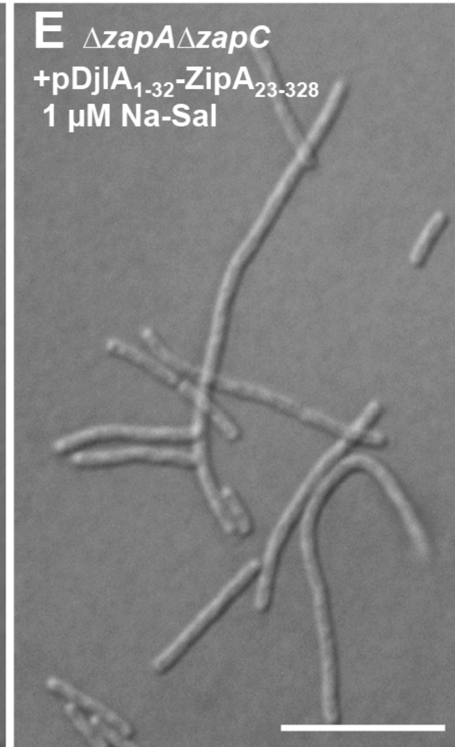

E ΔzapAΔzapC
+pDjlA1-32-ZipA23-328
1 µM Na-Sal

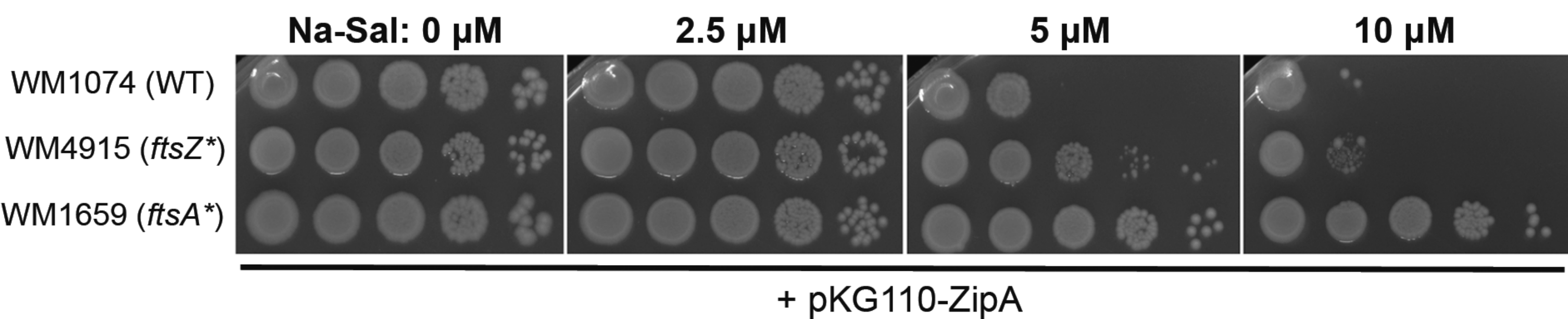
Na-Sal: 0 µM
2.5 µM
5 µM
10 µM
WM1074 (WT)
WM4915 (ftsZ*)
WM1659 (ftsA*)
+ pKG110-ZipA

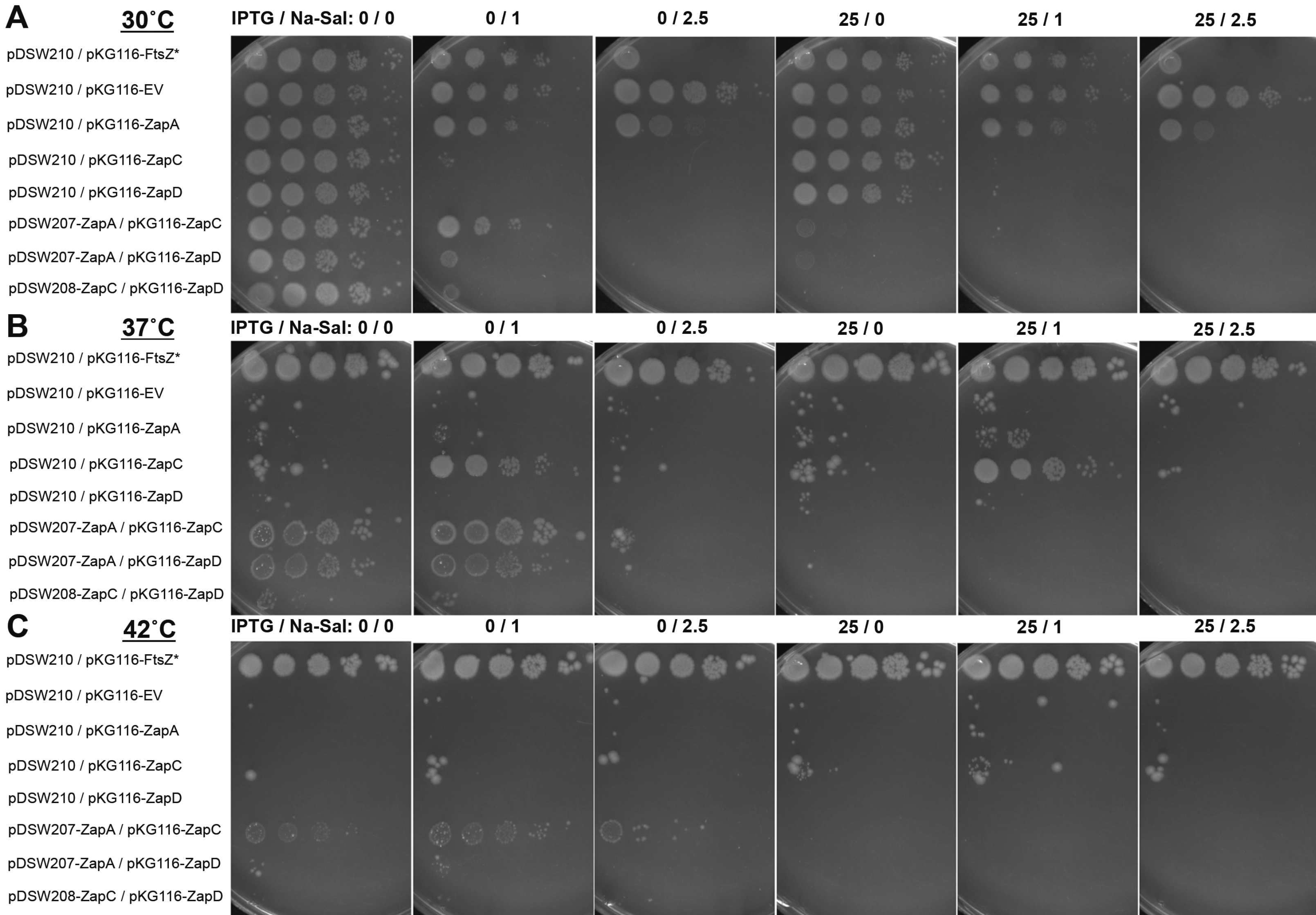
A
30˚C
B
37˚C
C
42˚C
IPTG / Na-Sal: 0 / 0
0 / 1
0 / 2.5
25 / 0
25 / 1
25 / 2.5
pDSW210 / pKG116-FtsZ*
pDSW210 / pKG116-EV
pDSW210 / pKG116-ZapA
pDSW210 / pKG116-ZapC
pDSW210 / pKG116-ZapD
pDSW207-ZapA / pKG116-ZapC
pDSW207-ZapA / pKG116-ZapD
pDSW208-ZapC / pKG116-ZapD

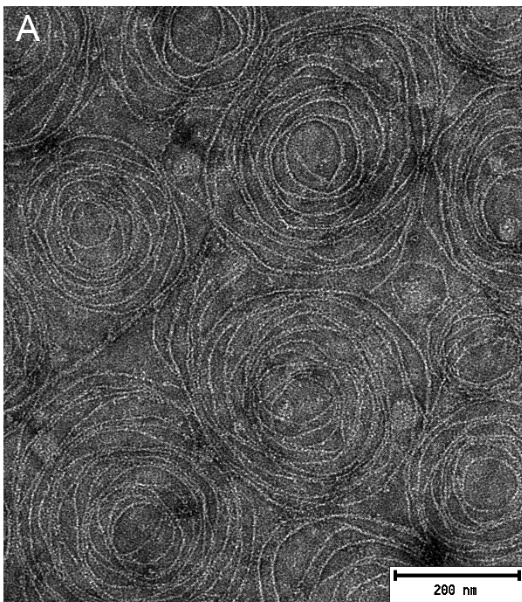
A
200 nm
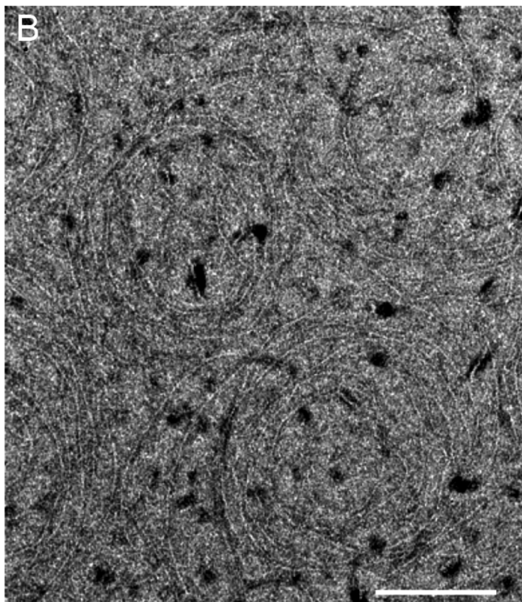
B
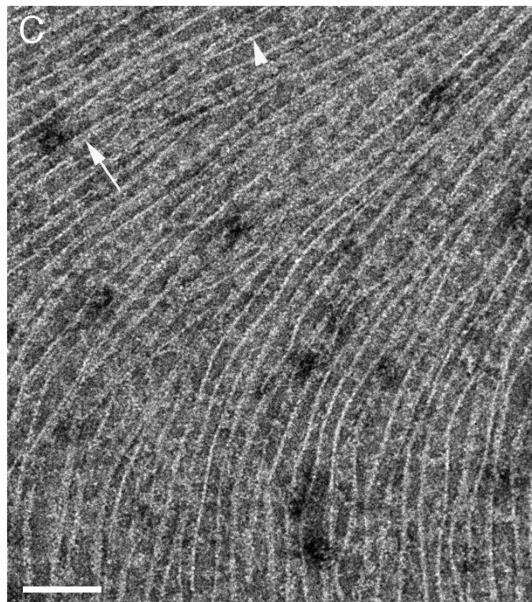
C

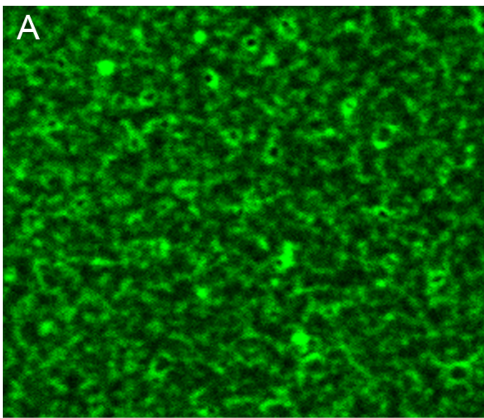
A
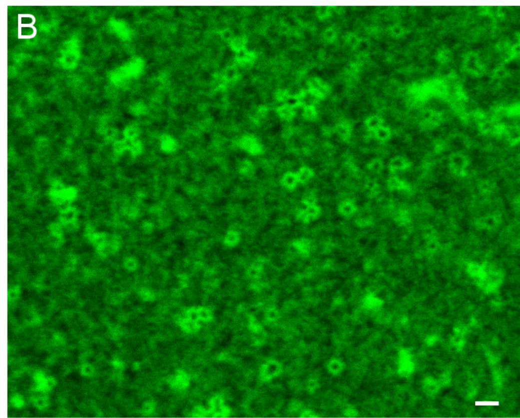
B
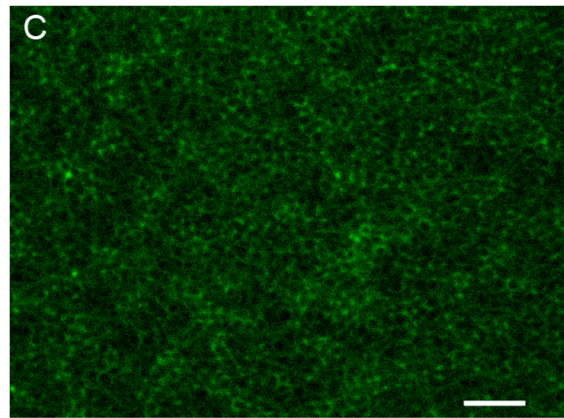
C